

Supplementary Materials for

Solvate ionic liquid derived solid polymer electrolyte with lithium bis(oxalato) borate as a functional additive for solid-state lithium metal batteries

Yan Yuan^{1,2*}, Xiuping Peng¹, Bin Wang¹, Kesi Xue¹, Zhengqian Li¹, Yitian Ma³, Bin Zheng³, Yonghui Song^{1,2}, Hai Lu^{3*}

¹School of Metallurgical Engineering, Xi'an University of Architecture and Technology, Xi'an 710055, China

²Shaanxi Key Laboratory of Gold and Resources, Xi'an 710055, China

³School of Materials Science and Engineering, Xi'an University of Science and Technology, Xi'an 710054, China

* Corresponding author 1#: Tel.: +86 29 82202923
E-mail address: lingshi21@126.com

* Corresponding author 2#: Tel.: +86 29 85587373
E-mail address: lhust@126.com

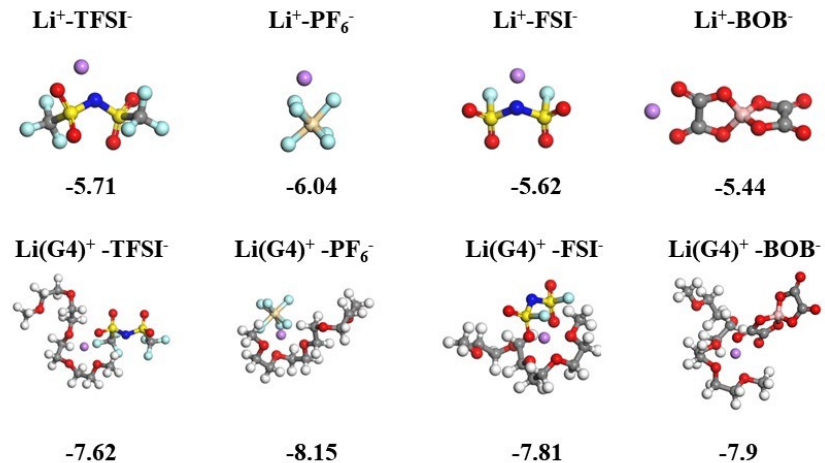


Fig.S1 Interactions of Li ion or solvated Li ion with various counteranions. The gas-phase binding energy for each configuration is expressed in eV.

Herein, a credible selection rule of the Li salt additive for the SIL-derived SPE can be concluded simply according to the order of binding energy (E):

- $E_{\text{Li-X}} > E_{\text{Li-TFSI}}$ and $E_{\text{Li(solvent)-X}} < E_{\text{Li(solvent)-TFSI}}$: LiX is easily dissociated and the resulted X^- is inclined to substitute for TFSI^- in the LIP.
- $E_{\text{Li-X}} > E_{\text{Li-TFSI}}$ and $E_{\text{Li(solvent)-X}} > E_{\text{Li(solvent)-TFSI}}$: LiX is easily dissociated but the resulted X^- is hard to substitute for TFSI^- in the LIP.
- $E_{\text{Li-X}} < E_{\text{Li-TFSI}}$ (usually $E_{\text{Li(solvent)-X}} < E_{\text{Li(solvent)-TFSI}}$): the dissociation of LiX and the resulted X^- could be limited, and/or the closely-contacted ion pair in IIP is mainly dominated by $\text{Li}^+ \text{-X}^-$ complex.

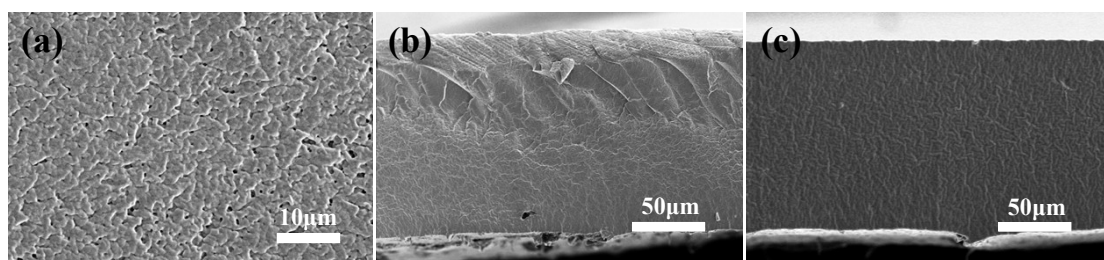


Fig. S2 (a) Surface and (b) cross-section SEM images of PVDF-HFP/LiTFSI; (c) Cross-section SEM images of PLGB

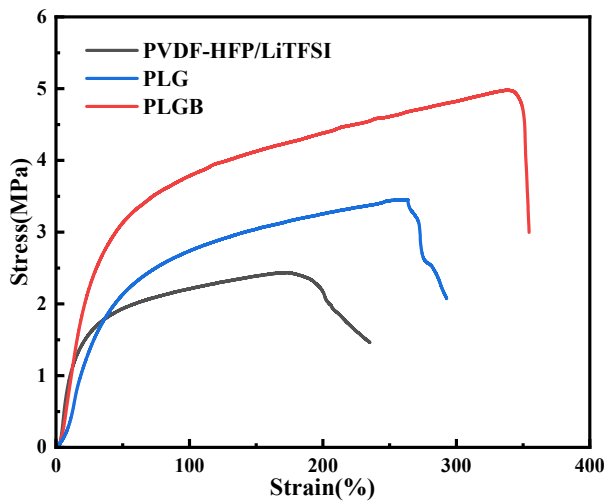


Fig. S3 Tensile stress-strain curves of various SPE films with the same thickness

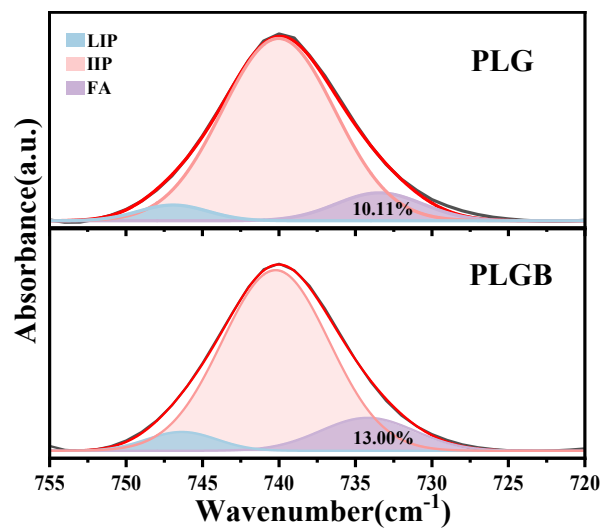


Fig. S4 Divided FTIR spectra of PLG and PLGB in the range of 755~720 cm^{-1}

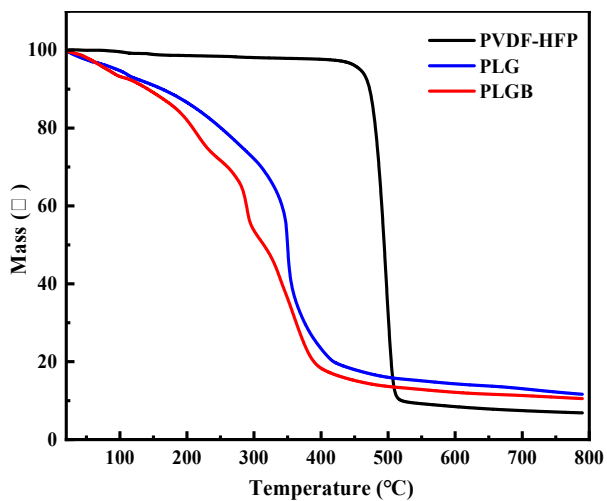


Fig. S5 TGA curves of pristine PVDF-HFP, as-prepared PLG and PLGB

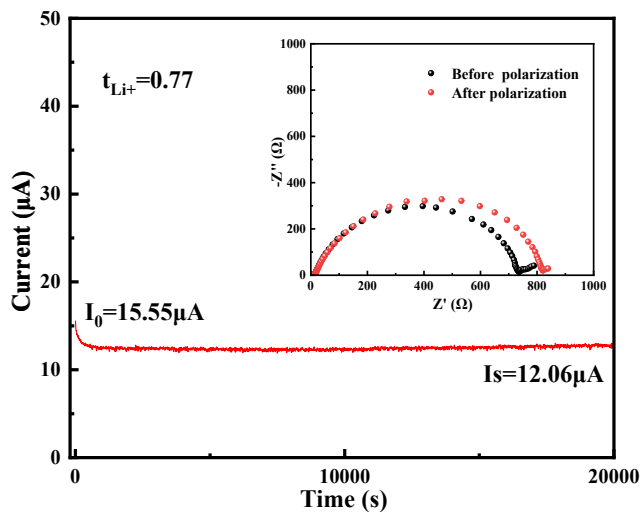


Fig. S6 Current-time curve of the symmetrical Li|PLG|Li cell obtained from chronoamperometry with an applied polarization voltage of 10 mV (the inset shows the Nyquist profiles before and after polarization)

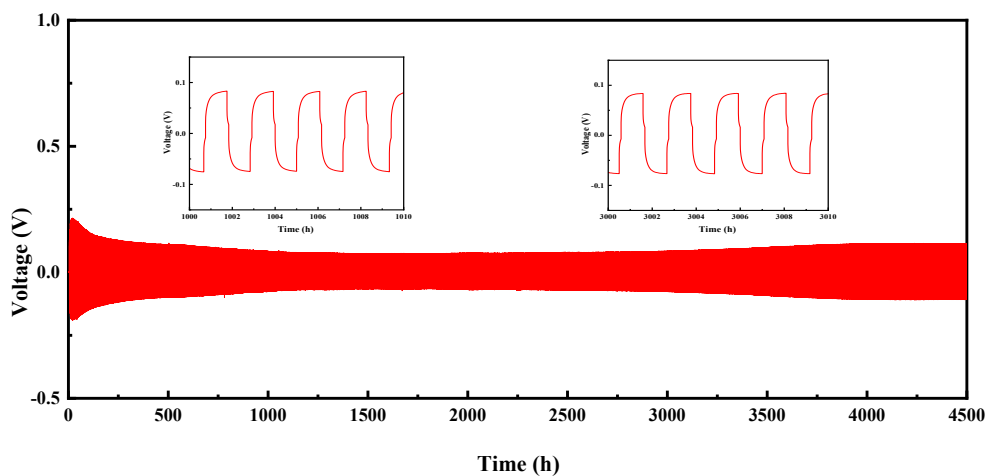


Fig. S7 Galvanostatic cycling profile of the symmetrical Li|PLGB-3|Li cell at the current density of 0.05 mA cm^{-2} at RT

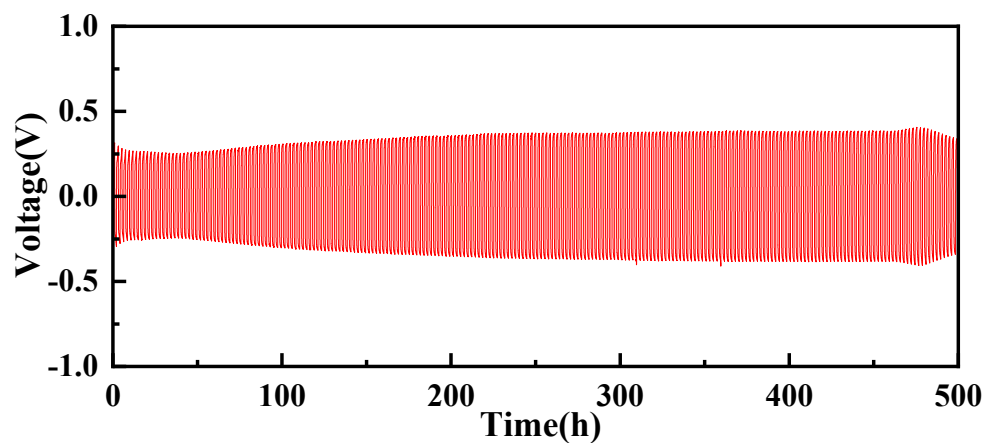


Fig. S8 Galvanostatic cycling profile of the symmetrical Li|PLGB-3|Li cell at the current density of 0.2 mA cm^{-2} at RT

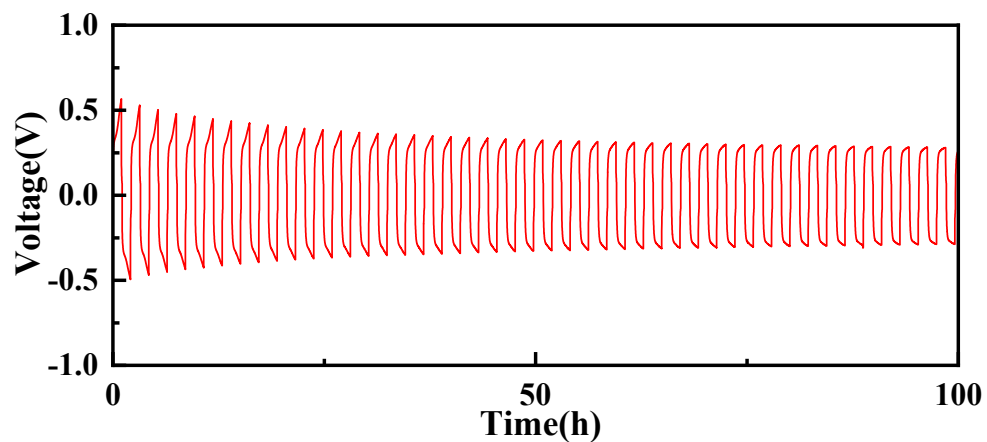


Fig. S9 Galvanostatic cycling profile of the symmetrical Li|PLGB-3|Li cell at the current density of 0.5 mA cm^{-2} at RT

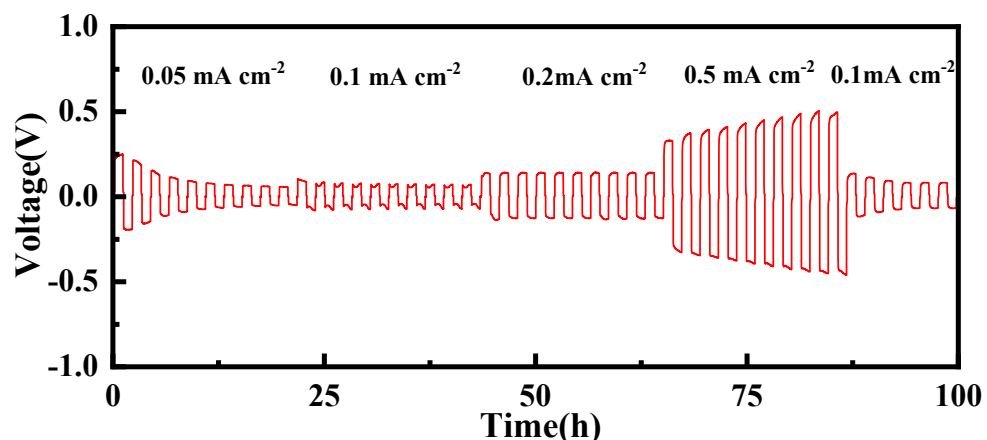


Fig. S10 Galvanostatic cycling profile of the symmetrical Li|PLGB-3|Li cell at various current densities

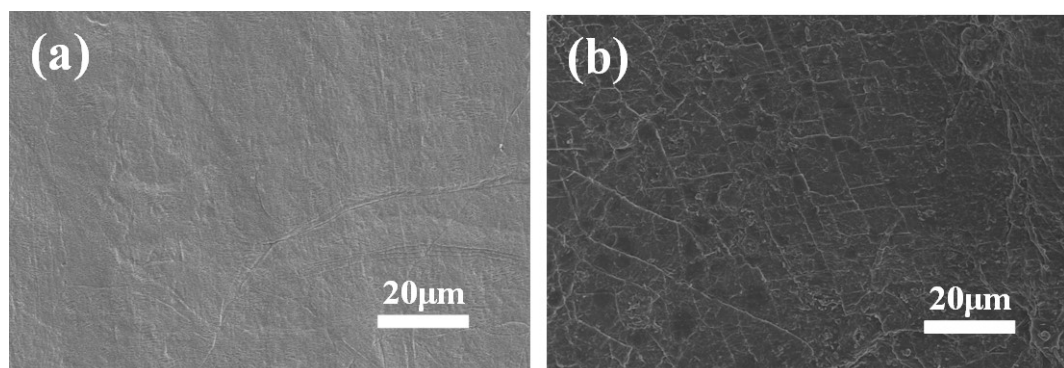


Fig. S11 SEM images of (a) fresh Li metal, (b) Li metal from the symmetrical Li|PLGB-3|Li cell after 2000h for Li stripping/plating at 0.1 mA cm^{-2}

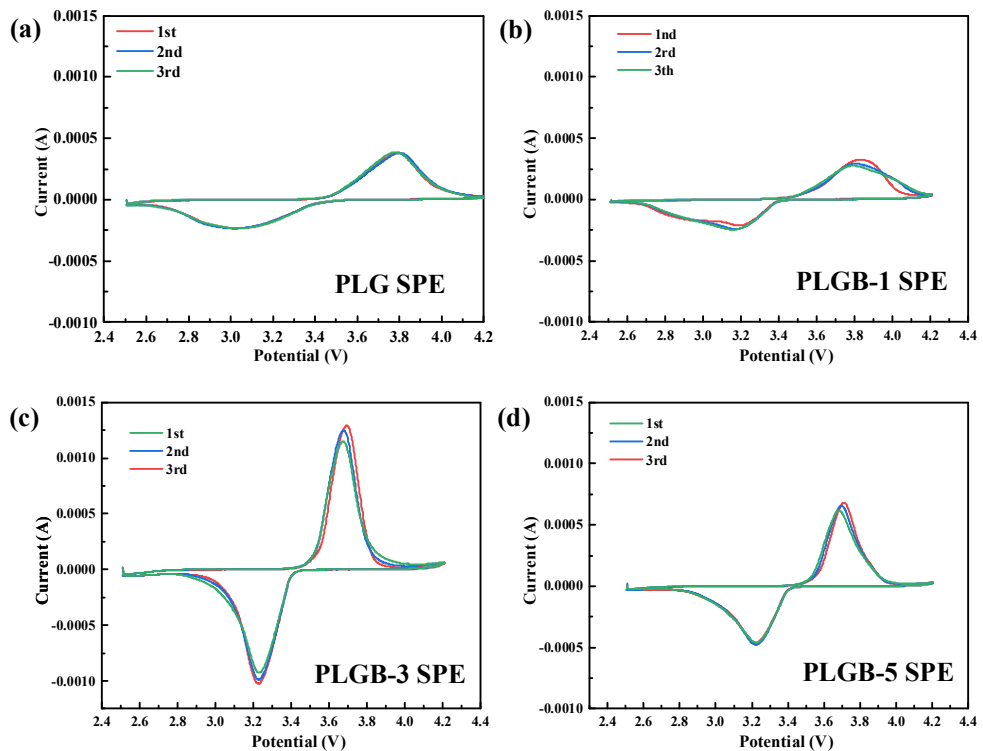


Fig. S12 CV curves of the LFP/Li cells with different SPEs

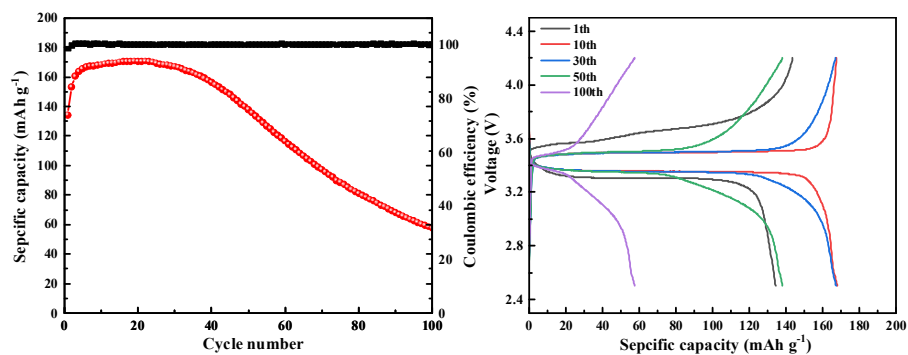


Fig.S13 Cycle performance of the LFP|PLG|Li cell at the rate of 0.1C

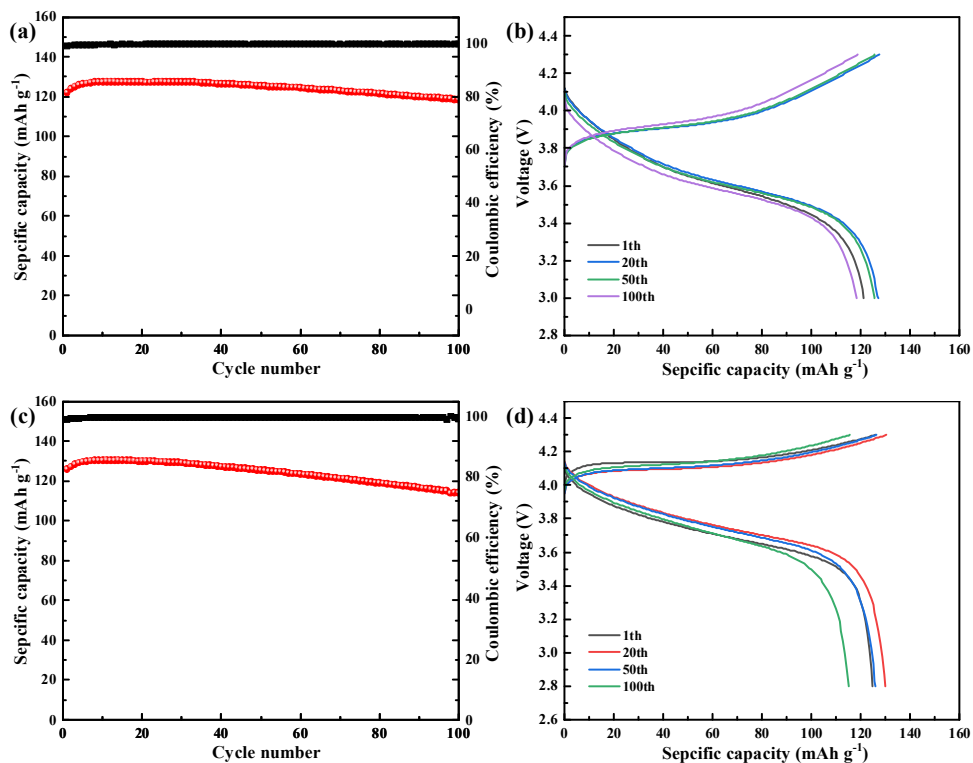


Fig. S14 (a) Cycle performance and (b) potential curves of NCM523|PLGB-3|Li cell at the current rate of 0.5C at RT; (c) Cycle performance and (d) potential curves of LCO|PLGB-3|Li cell at the current rate of 0.5C at RT

Table S1 Solvate species distribution proportion (%) in various liquid and solid electrolyte systems based on Raman spectra

Sample	Composition	FA	LIP	HIP
LG	[Li(G4) ₁][TFSI]	0	93	7
LGB	[Li(G4) ₁][TFSI]+LiBOB	3.72	87.42	8.79
PLG	[Li(G4) ₁][TFSI] / PVDF-HFP	7.90	87.73	4.37
PLGB	[Li(G4) ₁][TFSI]+LiBOB / PVDF-HFP	8.89	83.30	7.80

Table S2 Solvate species distribution proportion (%) in two solid electrolyte systems based on FT-IR spectra

Sample	Composition	FA	LIP	HIP
PLG	[Li(G4) ₁][TFSI] / PVDF-HFP	10.11	85.21	4.68
PLGB	[Li(G4) ₁][TFSI]+LiBOB / PVDF-HFP	13.00	81.37	5.63

Table S3 Overall comparison of the electrolyte properties and cell performances in previous reports

Electrolyte	σ /S cm ⁻¹ at RT	E_{ox} /V	t_{Li^+}	Performance	Ref.
PEO/HACCTFSI	1.9×10^{-7} (60 °C)	5.26	0.34	157 mAh g ⁻¹ , 100 th -98%, 0.2C, 60 °C	1
PEO/LLZO/SiO ₂ /Py ₁₄ FSI	7.4×10^{-4}	5.5		140 mAh g ⁻¹ , 100 th -96.4%, 0.1C, 25 °C	2
PEO/TiO ₂ /Li ₂ S ₆	1.7×10^{-4} (40 °C)		0.23	140 mAh g ⁻¹ , 700 th -80%, 0.2C, 50 °C	3
PEO/PEGDA/VMIMFSI	0.42×10^{-4}	5.44	0.22	147 mAh g ⁻¹ , 50 th -77.5%, 0.2C, 55 °C	4
PEO/LLZO/BMIMFFSI	2.2×10^{-4}	4.85	0.45	117 mAh g ⁻¹ , 150 th -84.1%, 0.1C, 25 °C	5
PVDF-HFP/DMF	3×10^{-4}	4.2	0.44	130 mAh g ⁻¹ , 200 th -95%, 0.2C, 25 °C (NCM111)	6
PEO/Li ₆ PS ₅ Cl/PP ₁₃ TFSI	1.12×10^{-4}			165 mAh g ⁻¹ , 50 th -89.1%, 0.18C, 25 °C	7
PEO/DME	1.09×10^{-3}	4.5	0.43	165 mAh g ⁻¹ , 300 th -79.2%, 1C, 60 °C (NCM111)	8
PVDF-HFP/BMIMSCN/CPT	1.9×10^{-4}			150 mAh g ⁻¹ , 50 th -76%, 0.06C, 25 °C	9
PVDF-HFP/G4/LiBOB	2.18×10^{-3}	5.7	0.86	143 mAh g⁻¹, 500th-95.9%, 0.5C, 25 °C	This work

- 1 J. Tan, X. Ao, A. Dai, Y. Yuan, H. Zhuo, H. Lu, L. Zhuang, Y. Ke, C. Su, X. Peng, B. Tian and J. Lu, *Energy Storage Materials*, 2020, **33**, 173.
- 2 Y. Zhai, G. Yang, Z. Zeng, S. Song, S. Li, N. Hu, W. Tang, Z. Wen, L. Lu and J. Molenda, *ACS Applied Energy Materials*, 2021, **4**, 7973.
- 3 R. Fang, B. Xu, N.S. Grundish, Y. Xia, Y. Li, C. Lu, Y. Liu, N. Wu and J.B. Goodenough, *Angew Chem Int Ed*, 2021, **60**, 17701.
- 4 Y. Li, Z. Sun, L. Shi, S. Lu, Z. Sun, Y. Shi, H. Wu, Y. Zhang and S. Ding, *Chemical Engineering Journal*, 2019, **375**, 121925.
- 5 H. Huo, N. Zhao, J. Sun, F. Du, Y. Li and X. Guo, *Journal of Power Sources*, 2017, **372**, 1.
- 6 Q. Liu, G. Yang, X. Li, S. Zhang, R. Chen, X. Wang, Y. Gao, Z. Wang and L. Chen, *Energy Storage Materials*, 2022, **51**, 443.
- 7 M. Liu, S. Zhang, E.R.H. van Eck, C. Wang, S. Ganapathy and M. Wagemaker, *Nat Nanotechnol*, 2022, **17**, 959.
- 8 H. Wu, Y. Xu, X. Ren, B. Liu, M.H. Engelhard, M.S. Ding, P.Z. El-Khoury, L. Zhang, Q. Li, K. Xu, C. Wang, J.G. Zhang and W. Xu, *Advanced Energy Materials*, 2019, **9**, 1902108.
- 9 J.C. Barbosa, D.M. Correia, E.M. Fernandez, A. Fidalgo-Marijuan, G. Barandika, R. Goncalves, S. Ferdov, V. de Zea Bermudez, C.M. Costa and S. Lanceros-Mendez, *ACS Appl Mater Interfaces*, 2021, **13**, 48889.